Insulation Materials and Systems for Power Electronics Modules: A Review Identifying Challenges and Future Research Needs

Boya Zhang[1], Mona Ghassemi[2] and Yunxiao Zhang[3]
[1]State Key Laboratory of Electrical Insulation and Power Equipment,
School of Electrical Engineering, Xi'an Jiaotong University, Xi'an, Shaanxi 710049, China
[2]Department of Electrical and Computer Engineering, Virginia Tech, Blacksburg, VA 24061, USA
[3]State Key Laboratory of Control and Simulation of Power Systems and Generation Equipment,
Department of Electrical Engineering, Tsinghua University, Beijing 100084, China

ABSTRACT

This manuscript critically reviews recent research on electrical insulation materials and systems used in power electronics devices and focuses on electrical treeing in silicone gel, PD modeling, and mitigation methods. For mitigation methods, electric field grading techniques, such as 1) various geometrical techniques, and 2) applying nonlinear dielectrics are discussed. Alternatives for silicone gel, such as liquid dielectrics, are also highlighted. The drawbacks of reported research and technical gaps are identified. In particular, we show that the investigations carried out to date are in their infancy regarding the working conditions targeted for next-generation WBG power devices. This review will provide a useful framework and point of reference for future research.

Index Terms — **insulation degradation, electrical tree, silicone gel, high temperature, high frequency, high slew rate, wide bandgap, power electronics modules**

1 INTRODUCTION

THE trend towards more and all electric apparatuses and more electrification will lead to a higher electrical demand. Increases in electrical power demand can be provided by either higher voltages or higher currents. Owing to weight and voltage drop, an increase in current is not preferred; thus, higher voltages are being considered. Another trend is to reduce the size and weight of apparatuses. Combined, these two trends result in the high-voltage, high-power-density concept.

It is expected that by 2030, 80% of all electric power will flow through power electronics systems [1]. In regards to the high-voltage, high-power-density concept described above, WBG power modules made from materials such as SiC and GaN (and, soon, Ga_2O_3 and diamond), which can tolerate higher voltages and currents than Si-based modules, are considered to be the most promising solution to reducing the size and weight of power conversion systems.

In addition to the trend towards higher blocking voltage, volume reduction has been targeted for WBG devices. The blocking voltage is the breakdown voltage capability of the device, and volume reduction translates into power density increase. For example, while the blocking voltage for commercial Si insulated gate bipolar transistors (IGBT) is 6.5 kV, the highest blocking voltage for SiC IGBTs is 15 kV for 80 A and 24 kV for 30 A [2]. Compared to the 6.5 kV Si-based solutions, the 15 kV SiC-based power module has one-third the volume, which translates into higher electric stress within the module. This leads to extremely high electric stress, E, within the module, leading to a higher possibility of partial discharge (PD) and, in turn, insulation degradation and, eventually, breakdown of the module.

One of the merits of WBG devices is that their slew rates and switching frequencies are much higher than Si-based devices. However, frequency and slew rate are two of the most critical factors of a voltage pulse, influencing the level of degradation of the insulation systems exposed to such pulses. For solid dielectrics used in electrical rotating machines, it was experimentally shown that the shorter the rise time, the larger the PD magnitude; thus, the shorter the lifetime [3–5, to cite a few]. Furthermore, lifetime decreases with increasing frequency. This will also be a problem for the silicone gel and ceramic dielectrics used in next-generation WBG power devices, as discussed in Section 2.3(b), because these insulators will experience high slew rates (dv/dt) (ranging from tens to hundreds of kV/μs) and repetitive (frequencies ranging from hundreds of kHz to MHz) voltage pulses. Also,

Manuscript received on 20 April 2020, in final form 18 June 2020, accepted 18 June 2020. Corresponding author: M. Ghassemi.

DOI: 10.1109/TDEI.2020.009041

Authorized licensed use limited to: to IEEExplore provided by University Libraries | Virginia Tech. Downloaded on December 03,2021 at 03:46:18 UTC from IEEE Xplore. Restrictions apply.

it should be noted that degradation mechanisms in silicone gel, as discussed in Section 2, are different from those for solid insulators used in electrical rotating machines.

WBG power devices also exhibit reduced conduction and switching losses and are able to operate at higher temperatures—up to 500°C has been targeted. This adds thermal stress on top of the two stresses mentioned above (i.e., high electric field and high slew rate, high frequency square wave voltages). It is expected that these three stresses will lead to accelerated aging and degradation of the insulation materials used in next-generation WBG power modules.

This manuscript critically reviews recent efforts and presents technical gaps and challenges for developing insulation materials and systems for next-generation WBG-based devices for power electronics modules. A thorough and in-depth review of PD measurements, failure analyses, and control in high-power Si-IGBT modules has been done by the second author [6, 7]. This paper discusses more recent research that was not reviewed in [6, 7]. Together, these three publications, [6, 7] and this paper, cover almost all electrical insulation issues and challenges to power electronics modules. To the best of our knowledge, such a critical review, that also identifies future research needs, has not been reported to date.

2 ELECTRICAL TREE DEGRADATION OF SILICONE GEL

Two common insulation materials used in power electronic modules are ceramic substrates and silicone gel. As the main insulation system, ceramic substrates ensure electrical insulation between active components and the baseplate, which is generally grounded. Silicone gel is used for encapsulation to prevent *in situ* electrical discharges in air and to protect substrates, semiconductors, and connections against humidity, dirt, and vibration.

Silicone gels are a special class of encapsulants that cure to an extremely soft material. Because of the wide angle variation of the Si-O-Si bonds, from 105° to 180°, the rotation is essentially free around these bonds [8] and the polymer network chains are very flexible, resulting in a large free volume within the polymer and low intermolecular interaction. Consequently, silicone gel acts as a two-component material that exhibits features of both a solid and a liquid. After curing, silicone gel results in a soft and resilient material that retains the stress relief and self-healing qualities of a liquid while providing the dimensional stability of a cross-linked elastomer. The self-healing nature of silicone gels allows any damage that occurs when it is subjected to mechanical stress or PDs involved in electrical treeing to recover. Moreover, the physical and electrical stability of silicone gel can be maintained over a wide temperature range from -45°C to 200°C [8]. The naturally sticky surface also allows silicone gels to gain adhesion to most common surfaces without the need of primers. Therefore, all these special features make silicone gels the most effective encapsulants for power electronics devices.

Electrical treeing, which is a well-known electrical pre-breakdown phenomenon and a damaging process due to PDs in solid insulation, has also been observed in silicone gels. However, compared to solid dielectrics, the low number of manuscripts dealing with electrical treeing in silicone gel shows that this topic is immature. In the following sections, the general features of electrical treeing degradation resulting from PD activities in silicone gel are reviewed, the technical gaps are identified, and future research needs are highlighted.

2.1 MORPHOLOGIES OF ELECTRICAL TREEING IN SILICONE GEL

The study of electrical tree degradation in solid dielectrics dates back a hundred years. Experiments were conducted in various insulating polymers, including rubber, polyethylene, and epoxy resin [9–11, to cite a few]. Most of these studies focused on tree initiating dynamics and their morphologies. The morphologies of electrical trees provide the most favorable basis for revealing the degradation mechanisms in different materials because the growth of an electrical tree highly depends on the material's crystal structure and molecular segments [12, 13], which changes with external conditions [14].

Due to the flexible polymer network chains as explained above, silicone gel possesses a unique two-phase liquid-solid nature, which makes the tree morphologies in silicone gel very different from solid materials. It was shown that under AC voltage, there is a filamentary branched component of trees in silicone gel that is retained after the electrical field is removed, like in solids, as well as bubble-like cavities that expand, become isolated, and collapse during growth, like streamers in liquid [8, 15].

This phenomenon was analyzed in detail in a fascinating experiment performed on a range of samples made by varying the ratio of two liquid components (A and B) used for cross-linking a commercial silicone gel [16]. As shown in Figure 1a, the regions at <40% A and >95% A correspond to a liquid phase, where the sample behaves more like a high viscous liquid than an elastic solid. Maximum hardening appears at 66–70% A, resulting in a rubbery-like elastomer due to the maximum efficiency of the cross-linking reactions between components A and B. In between the liquid and the elastomer phases are gel-like products (i.e., around 50% A and 85% A), whose real component of elastic shear modulus, G', is two orders of magnitude smaller than the value of the elastomer.

The electrical treeing behaviors of different compositions are shown in Figure 1b. In the liquid region, only streamers are grown, while in the elastomer region, only branched tree structures that are similar in form to those found in other solid dielectrics are observed (Figure 1b-III). This kind of tree suffers from irreversible chemical changes such as chain scissions and further carbonization, so the structure is retained after the removal of the applied voltage.

Gel samples exhibit treeing behavior that includes features typical of both liquids and solids, and show different self-healing mechanisms depending on the degree of curing. Near

Authorized licensed use limited to: to IEEExplore provided by University Libraries | Virginia Tech. Downloaded on December 03,2021 at 03:46:18 UTC from IEEE Xplore. Restrictions apply.

the gel-liquid boundary with 45% A (Figure 1b-I), a fast streamer channel of more than 1 mm length formed within 3 minutes and started to disappear in 1/20 s later. Then, a complete and fast self-healing behavior on the order of microseconds to tenths of a second was observed. This behavior during voltage application can be regarded as the first self-healing stage.

At the manufacturer's recommended composition, i.e., gel sample with 50% A (Figure 1b-II), the growth of electrical trees involved the formation of near-spherical cavities on the tips of the filaments. These cavities in gels are, in fact, slow streamers with shorter and wider dimensions compared to those found in liquids [17–19]. They expand, collapse, and disappear, as do such cavities in liquid breakdown structures [18, 20, 21], on a timescale of a few seconds through the same mechanism as the first self-healing stage. However, the repetition of discharges makes the cavities stable. These new quasi-permanent cavities add to the fractal trees that are the backbone of the degradation structure. Unlike more rigid dielectrics, such as epoxy resin and polyethylene, the flexible elastic nature of the gel allows the structure to contract and gradually fade once the voltage is removed [8]; this is known as the second stage of self-healing.

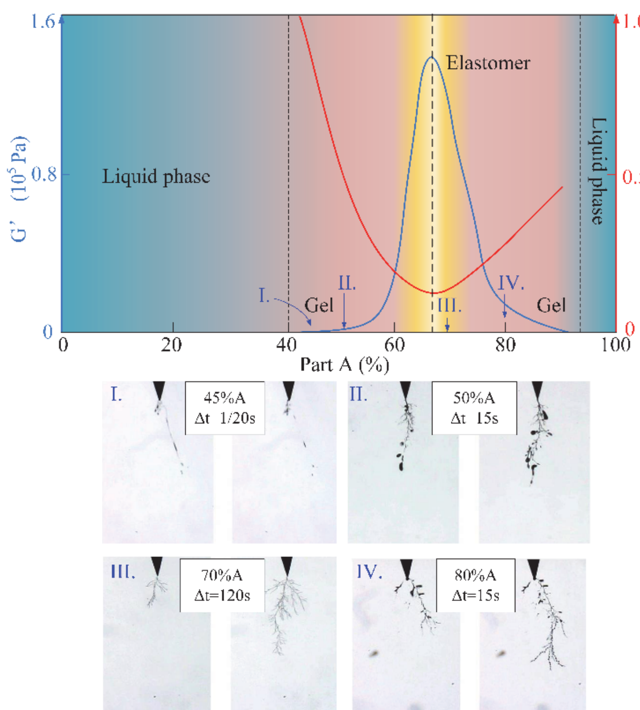

Figure 1. (a) Real component of the elastic shear modulus, G', (blue line) and loss tangent, $\tan\delta$, (red line, $\tan\delta = G''/G'$ where G'' is the imaginary component of the elastic shear modulus) after completion of the curing process at 65°C as a function of the concentration of A; (b) Comparison of electrical treeing morphologies of cured samples with different ratios of components [16], © [2016] IEEE.

It should be noted that silicone gel is not a liquid so its self-healing capability is not unlimited. Some filamentary structures can be retained if the gel suffers from repetitive discharges. This can be regarded as a form of irreversible degradation such as observed in [22, 23].

2.2 DYNAMICS OF ELECTRICAL TREEING IN SILICONE GEL

As discussed above, the tree morphologies in silicone gels are generally bubble cavities along the filamentary branches. This hybrid structure is similar to those grown from negative needles in liquids [24, 25]. In [26], researchers observed that electrical treeing in silicone gel starts on the negative half-cycle of an AC voltage with the formation of bubble cavities. This is retained in the following cycles and rapidly extends into the material in the form of a streamer. It is presumed that the initial electron injection heats the liquid component allowing vaporization and the formation of cavities capable of supporting gas discharges within themselves to occur. It has also been suggested that the formation of cavities is expected as a result of equilibration between the internal gas electrostatic pressure and the external liquid-phase hydrostatic pressure [16], just like in liquids [20, 21].

A more fundamental mechanism was proposed in [27, 28] for the dynamics of electrical treeing in silicone gel. It was determined by carefully observing the motion of the trees during discharges on a substrate and by calculating the stress exerted on the cavity surface. The temporal response of the stress was quantitatively calculated based on the constitutive equation of viscoelasticity [29], where the response depends on the location of the cavity—whether it is at the tip of the trees or adjacent to the electrode.

For cavities formed at the tip of the trees, Figure 2 shows their typical structures under AC voltage and the relationships among the applied voltage, apparent charge of PDs, and the diameter of the cavities [27]. It is clear that PD pulses can be identified at the same time that their diameters fluctuate steeply. Whenever PD occurs, it should increase the pressure within the cavity; PD (iii) and PD (vii), however, lead to a drop in the diameter of each cavity. In [28], similar results were observed and they revealed that the stress exerted on the cavity surface increased with some PDs and dropped with other PDs. Therefore, it was justified in [27, 28] that the change in cavity diameter should be driven by the electrostatic force due to charge accumulation on the surface of the cavities instead of the pressure increase due to gas discharges. The experimental results also revealed that the positive PD charge accumulating at the tip of the trees was larger than the negative one, which was attributed to the difference in the propagation length of surface discharge under different polarities.

For cavities adjacent to the electrode, Figure 3 shows the relationships among the applied voltage, the apparent charge of the PDs, the diameter of the cavities, and the stress being exerted on the cavity surface as well as an image of the cavity. It can be seen that the waveform of the diameter lags the stress waveform, which is due to the viscosity of the gel. The stress changed as the second harmonic of the applied voltage waveform with a $\varphi = \pi/2$ advance in phase. This indicates that the conductivity of the cavity near the electrode is high because conducting fragments of molecules accumulate on the cavity surface [29].

Authorized licensed use limited to: to IEEExplore provided by University Libraries | Virginia Tech. Downloaded on December 03,2021 at 03:46:18 UTC from IEEE Xplore. Restrictions apply.

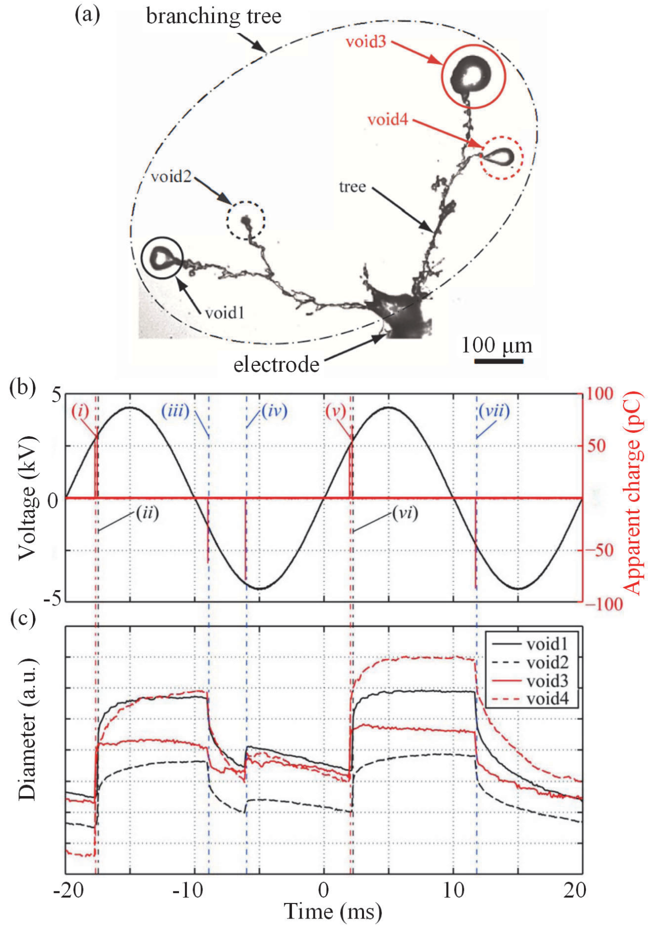

Figure 2. (a) Image of branching trees and the formation of voids at the tip of the cavity, (b) The relationship between applied voltage, the apparent charge of PD, and (c) diameter of the void (for two cycles) [27], © [2014] IEEE.

The dynamics of the electrical treeing in silicone gels was further explored by measuring the dynamic change of potential distributions during surface discharge at the gel-substrate interface using the Pockels technique [30, 31] where the measured potential directly revealed the amount of accumulated charge on the cavity surface. It was found that when PDs occur, the diameter of voids and the potential close to the cavities fluctuate steeply. Also, the fluctuation of cavity diameter coincides with the fluctuation of the potential. The above observations confirmed that conductive streamers initiate at the electrode, propagate towards the cavity, and accumulate charges on the cavity surface. Meanwhile, the motion of the cavity is driven by the change of electrostatic force due to the absolute value of the net charge within the cavity.

All justifications mentioned above are qualitative and may not work for other test conditions (different applied voltage waveforms; different electrode materials and geometries; and different gap distances). Indeed, as the first technical gap, we still don't have enough experimental data from different conditions or even for the same conditions—the test results from one laboratory may be different from those of other laboratories. Physical-based theoretical models must be developed to understand the mechanisms and phenomena behind electrical tree degradation. Without such models, we cannot adequately examine the influence of various mechanisms and phenomena, and of course, the development of such models, as the second technical gap, is challenging and complicated.

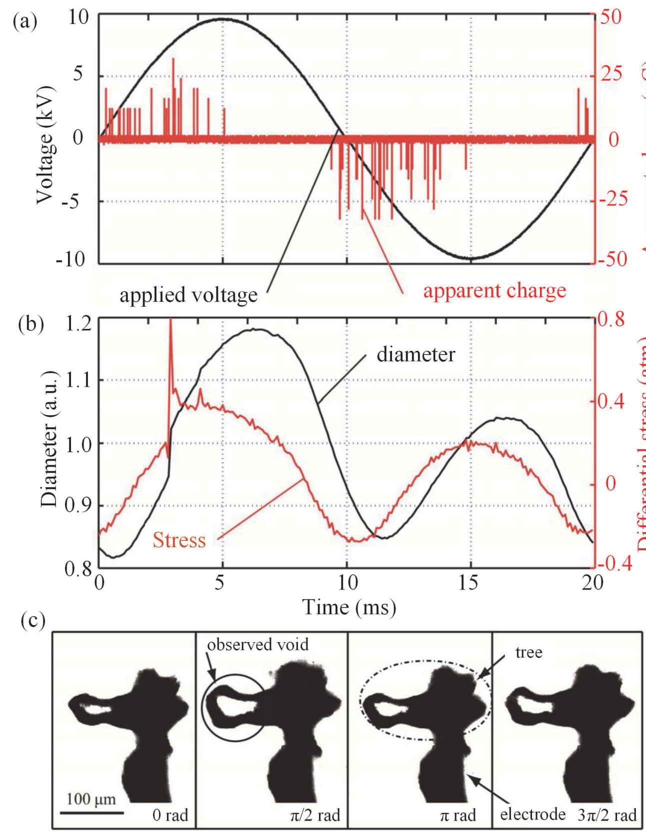

Figure 3. The relationship between (a) applied voltage, the apparent charge of PD, and (b) void diameter and stress exerted on the void surface, (c) motion of the void observed near the electrode [27, 28], © [2014] IEEE.

2.3 INFLUNCE FACTORS ON ELECTRICAL TREEING BEHAVIOR

In general, the characteristics of electrical treeing behaviors are greatly affected by external conditions. So far, effects of voltage waveform, temperature, humidity, radiation, etc. have been considered for treeing behaviors in different polymers [32–34, to cite a few].

Unlike conventional insulation materials used in 50/60 Hz AC power frequency or DC situations, the silicone gel applied in high-power-density WBG power devices suffers from both high repetition square wave voltages (targeted up to MHz) and high operating temperatures (targeted up to 500 °C). Moreover, the insulation structure is unique since electrical treeing usually propagates along the surface of a ceramic substrate. Three factors—temperature, voltage waveform and frequency, and substrate—need to be carefully considered when studying the electrical tree behaviors of silicone gel.

***(a) Effect of Temperature*:** To the best of our knowledge, the temperature effect on insulation degradation, especially on electrical treeing degradation, in silicone gels has not been

Authorized licensed use limited to: to IEEExplore provided by University Libraries | Virginia Tech. Downloaded on December 03,2021 at 03:46:18 UTC from IEEE Xplore. Restrictions apply.

studied to date. There is a challenging technical problem where the operating temperature of silicone gel is limited to 200 °C. This means that for higher temperatures, new dielectrics or adding fillers to the silicone gel to increase the limit above 200 °C should be investigated.

However, even up to 200 °C, we need to know the influence of temperature on electrical treeing degradation in silicone gel. In this regard, other insulation materials have revealed that temperature has a great effect on both electrical tree initiation and propagation.

In principle, electrical tree initiation is associated with charge carrier injection and follows the law of Fowler-Nordheim emission, which is temperature-independent [35]. Thus, the effects of temperature on the amount of charge injection are limited. However, a rise in temperature will increase the free volume of the polymer [36], resulting in a longer free path for the injected electrons and greater energy accumulation before a collision, so it is easier to initiate tree degradation at higher temperatures [37].

For tree propagation, the severity of PDs and the destruction of tree channels determine the growth rate and morphology of the electrical tree. At higher temperatures, many observations have shown that denser bush-like trees are more likely to be formed [10, 33]. On the one hand, the amount of PD will increase as the temperature rises, thereby accelerating tree growth rate [34]. On the other hand, higher temperature leads to chain relaxation and larger free volumes in the material, which also facilitates tree propagation [38]. In addition, carbonization in tree channels can be observed under excessively high temperatures, which causes investable degradation in polymers [12].

Since silicone gel has a relatively higher conductivity and unique self-healing capability compared to conventional dielectrics, its treeing behavior under high temperatures may be different and, as mentioned before, we do not know enough about it.

(b) Effect of voltage waveform and frequency: Electrical tree initiation in silicone gel for sinusoidal and square voltages as a function of the frequency applied was studied in [15]. It was found that a square waveform exhibits a much lower tree inception voltage (TIV) than a sinusoidal waveform at the low frequency of 1 Hz. However, the TIV at 1 kHz was almost the same for both sinusoidal and square waveforms, as shown in Figure 4a.

Experiments further demonstrated that the reduction of TIV for the square waveform compared to the sinusoidal waveform was not due to the longer time spent at the maximum voltage, but, instead, to the shorter rise time of the voltage. Figure 4b shows the TIV of samples under a square voltage with two different slew rates. Under the same frequency, a higher slew rate leads to lower TIVs. In other words, the rise time is the most critical parameter that influences tree inception in silicone gel; in conventional solid materials, frequency is more relevant. Therefore, it was concluded that tree inception in gels is due to a single high energy event that forms a gas-filled cavity, in contrast to what is commonly known for solids where damage accumulation takes place.

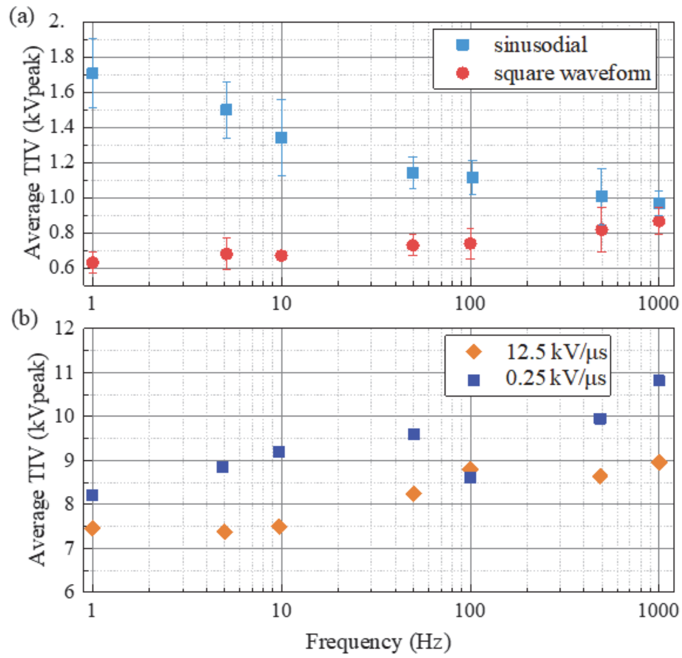

Figure 4. (a) Average TIV for silicone gels with a 3 μm-tip needle under sinusoidal and square waveforms; (b) Average TIV for silicone gel samples with a 5 μm-tip needle with 0.25 kV/μs and 12.5 kV/μs slew rate square voltage [15], © [2017] IEEE.

Here, the technical gaps are: 1) Both frequency and slew rate of square wave voltages tested to date (1 kHz and 12.5 kV/μs) are much lower than present and targeted values (up to MHz and hundreds of kV/μs) for WBG power modules; 2) All justifications, for example those mentioned above, are qualitative. Even models developed in [15] for electrical treeing inception are based on simple assumptions and hypotheses, not on fundamental (first principle) physics. Hypotheses were considered so that simulation results from the model were in good agreement with the test results for a specific test condition and setup. However, since the models are not based on fundamental physics, they may not work for other geometries and conditions, especially for the high frequencies and slew rates mentioned in 1); 3) Moreover, some test results are questionable. For example, regarding the trend before and after the frequency at 100 Hz in Figure 4b, it is crystal clear that the experimental part is immature and much more testing, especially carried out in different laboratories, is needed for us to be able to trust the test results.

The frequency and rise time of the applied voltage will also influence the dynamics of electrical treeing in silicone gel [39–41]. Attention was paid to the cavity length under repetitive voltage pulses. It was found that cavity length increases with frequency. This is easy to understand because cavities propagate more easily if subsequent discharges arrive before the discharge track heals. The cavity length is especially long when the rise time is short and the frequency is high, as shown in Figure 5.

Authorized licensed use limited to: to IEEExplore provided by University Libraries | Virginia Tech. Downloaded on December 03,2021 at 03:46:18 UTC from IEEE Xplore. Restrictions apply.

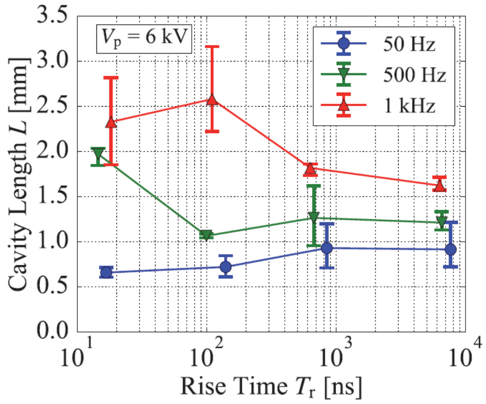

Figure 5. Rise time and frequency dependence of cavity length under bipolar repetitive voltage impulses [41], © [2019] IEEE.

When the rise time is short, PD occurs at a higher voltage due to its statistical time lag, and a longer and thicker discharge is formed. If it requires a longer time for a thicker discharge to heal, the occurrence of such a thicker discharge channel leads to further cavity propagation, as shown in the schematic model in Figure 6. The observation also showed that the discharge track has a filamentary-shape under positive impulses and has a spindle-shape under negative impulses.

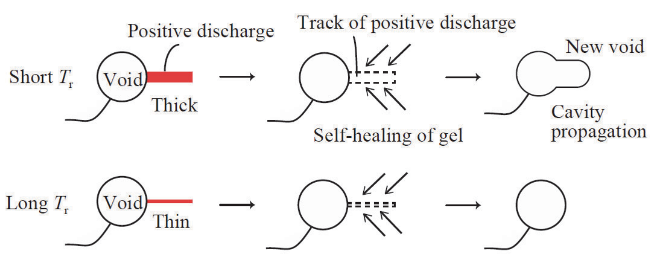

Figure 6. Cavity propagation models with different rise time (T_r) of the applied impulse voltage [41], © [2019] IEEE.

All three technical gaps mentioned above are also present here. For example, there are doubts about the accuracy of the test results shown in Figure 5 at around 100 ns for 500 Hz and 1 kHz.

To the best of our knowledge, the maximum frequency studied for electrical treeing degradation in the literature only reaches 130 kHz [42] and this was for silicone rubber (a solid dielectric) and not for silicone gel. It was observed that electrical trees tend to be denser and larger with rising frequency; when the frequency exceeds 100 kHz, bubble breakdown occurs in a very short time, as shown in Figure 7. It was claimed that this is mainly because extreme high frequency leads to much higher energy generated by the abundant charge carrier collisions, which directly causes destruction of the material and generates a large amount of gas until breakdown. Here, these justifications are also qualitative and may not be correct. Also due to the self-healing capability of silicone gel, results may be totally different.

(c) Effect of substrate: It was found that PD patterns in ceramic substrates embedded in a gel are different from those in the gel alone, and that changing the substrate material has a considerable effect on the PD features [43]. It was concluded that PDs of low amplitudes probably originate from the ceramic itself due to the presence of numerous µm-sized pores in sintered materials, as shown in Figure 8.

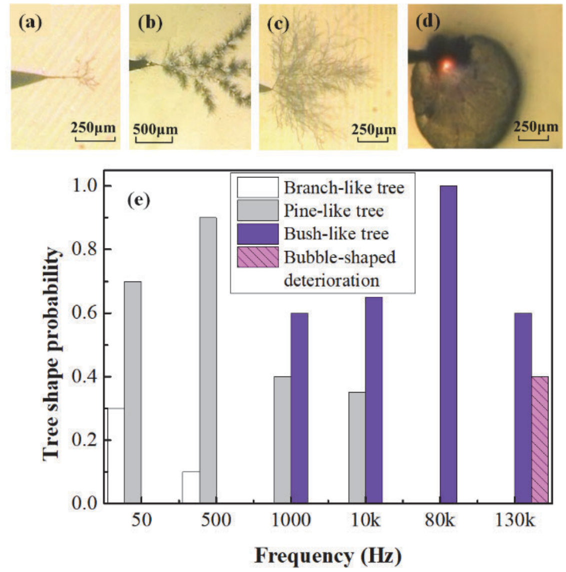

Figure 7. Electrical tree morphology and probabilities in silicone rubber under different frequencies. (a) branch-like tree; (b) pine-like tree ((a) and (b) for $50\ \text{Hz} \leq f \leq 500\ \text{Hz}$); (c) bush-like tree (for $f \geq 1\ \text{kHz}$); (d) bubble-shaped deterioration (for $f = 130\ \text{kHz}$); (e) tree morphology probabilities for different frequencies [42], © [2018] MDPI.

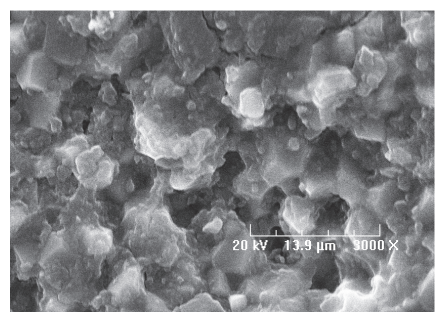

Figure 8. Image of the AlN surface observed by scanning electron microscopy [43], © [2013] IEEE.

The influence of different substrate material embedded in silicone gel was also investigated in [44]. It was found that the length of electrical trees in an AlN substrate is more than twice that on Al_2O_3 and glass substrates. Its light emission, due to surface discharges, showed discontinuity along the treeing path. The longer length of trees on the AlN substrate makes the surface of the AlN substrate degrade with repeated discharges and becomes conductive.

3 PD MODELING FOR AIR-FILLED CAVITIES IN SILICONE GEL

Although much work has been done and significant progress has been made on PD measurement and detection techniques, this is not the case for PD modeling. Four types of internal PD modeling, in sequential order from first to last developed, are three-capacitance (abc), induced charge

Authorized licensed use limited to: to IEEExplore provided by University Libraries | Virginia Tech. Downloaded on December 03,2021 at 03:46:18 UTC from IEEE Xplore. Restrictions apply.

concept (ICC), finite element analysis (FEA), and Multiphysics models.

The abc model, initiated by Whitehead [45], presents an equivalent circuit, including three capacitances, to model the void inside an insulating material. This model is too simple to provide an understanding of the physical phenomena affecting PD.

In contrast, Multiphysics models are immature. To the best of our knowledge, there are only two journal articles that used Multiphysics modeling for internal PD modeling [46, 47]. The low number of papers on this topic and their publication year (2018, 2019) indicates that this topic is very complex and immature. Multiphysics models need more physical parameters to be experimentally determined than other models, which is not a trivial task. Moreover, adjusting the physical parameters to achieve good agreement between simulation results and measurement results for a specific geometry and dimension may not work for other geometries and dimensions.

The FEA model, a relatively recent model [48–50, to cite a few], and the ICC model [51, 52, to cite a few], fall between the abc and Multiphysics models in terms of modeling complexity, and can partly explain mechanisms and physical phenomena associated with internal PDs.

However, all PD modeling developed to date are for cavities inside solid dielectrics and not for silicone gel. To the best of our knowledge, there is only one paper [53] that developed an FEA approach for PD modeling in a void located in silicone gel under fast rise time, high frequency voltage pulses. Figures 9a and 9b show the case study that consists of a sphere-sphere electrode system that provides a weakly nonuniform electric field embedded in silicone gel and a spherical air-filled cavity that is located between the electrodes. The electric field distribution is shown in Figures 9c and 9d right before and right after PD occurrence. As expected, the electric field intensity inside the cavity is higher than the surrounding material, and it increases up to a point where the cavity can no longer withstand the electric stress. Figures 9e and 9f show the destructive impact of frequency and rise-time on PD charge magnitude.

In the FEA model, developed in [53], COMSOL Multiphysics was integrated with MATLAB. All equations for streamer inception criterion and initial free electron generation were coded in MATLAB while the electric field calculations were carried out in COMSOL Multiphysics. Such FEA PD models have also been developed for fast rise time, high frequency square waveform applied voltages, but were for an air-filled cavity in a solid dielectric in [54, 55].

The technical gaps and challenges here are:

1) The only research conducted on internal PD modeling in an air-filled void embedded in silicone gel is [53]. It is crystal clear that much more research is needed to elucidate the mechanisms behind prebreakdown in silicone gel. Moreover, it should be noted that the adjustment of PD model parameters done under 50/60 AC sinusoidal voltage or frequencies up to 100 Hz [50] may not valid for high slew rate, high-frequency square wave voltage pulses.

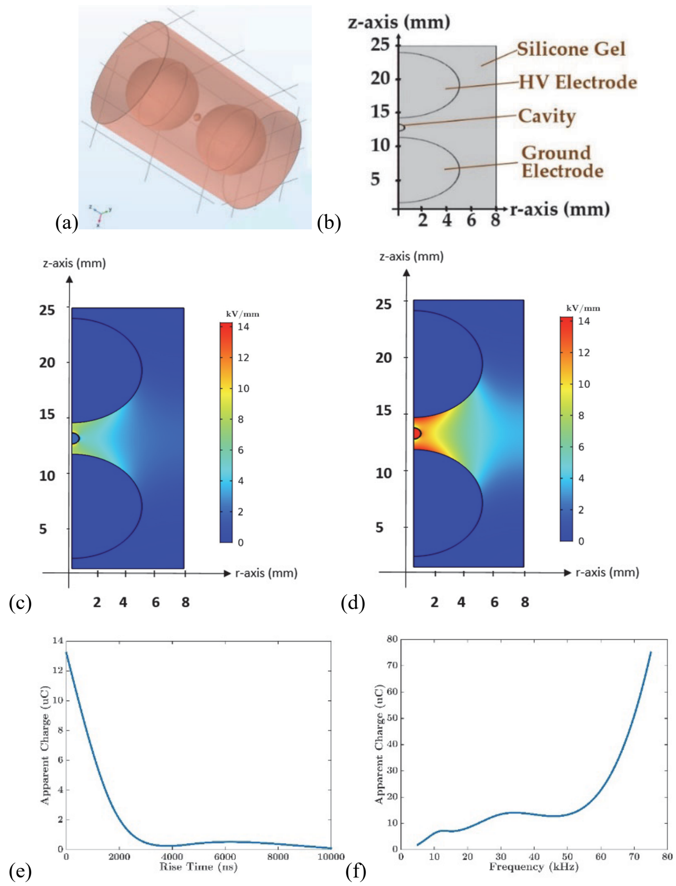

Figure 9. (a) 3D representation, (b) 2D FEA model, the electric field distribution (c) before, and (d) after PD, the impact of (e) frequency, and (f) rise-time on PD intensity [53], © [2019] MDPI.

2) The FEA model developed in [53] is for a weakly nonuniform electric field because the model parameters needed to be adjusted with the experimental data for a similar electrode geometry. Moreover, the model is also valid for only the specific frequency of the square waveform applied voltage. In other words, we do not know whether Figures 9e and 9f are reliable or not since these simulation results need to be validated with experimental results.

Furthermore, we do not know what the simulation and experimental results are for extremely nonuniform electric fields, which are closer to the situation within power modules regarding sharp edges of metallization layers and protrusions. In this regard, basic research is needed to address this lack of knowledge. Different setup arrangements should be designed including (1) sphere-sphere, (2) needle-plane, (3) needle-sphere electrode geometries, and (4) ceramic substrates made of (a) AlN, (b) Al_2O_3, and (c) glass/epoxy, embedded in silicone gel. Both AC 60 Hz and square waveform voltages should be applied. For the square waveform voltage, the influence of frequency and slew rate on PD parameters including (a) PD pattern, (b) PD magnitude, (c) PD repetition rate, and

Authorized licensed use limited to: to IEEExplore provided by University Libraries | Virginia Tech. Downloaded on December 03,2021 at 03:46:18 UTC from IEEE Xplore. Restrictions apply.

(d) endurance (lifetime) and electrical treeing parameters need to be investigated.

3) If the mechanism of electrical failure in solid insulation is not fully understood, comparatively, we know almost nothing about silicone gels. The efforts reported in [53] may be regarded as very preliminary results for insulation degradation modeling in silicon gels. Indeed, there is a long way to go before we are able to model the electrical treeing behaviors discussed in Section 2 as 2D and 3D simulations.

4) As mentioned in Section 2, experimental investigations do not include the impact of thermal stress. If such experimental data was available, then modeling and simulation of very complex physical phenomena that consider the electric field coupled with high-temperature impact and its extremely nonuniform distribution will be very challenging.

4 MITIGATION METHODS

In this section, the mitigation methods proposed to date to address the accelerated insulation degradation issue in next-generation WBG-based power modules are critically reviewed, and technical gaps and future research needs are identified and highlighted.

Four solutions have been proposed for electric field reduction and PD control within envisioned high voltage, compact packaging design of power modules: 1) geometrical techniques [56–60], 2) applying nonlinear field-dependent conductivity (FDC) materials as coatings on high field regions [61] or field-dependent permittivity (FDP) fillers in silicone gel [62], 3) using high-temperature (up to 350°C) insulating liquids as a potential replacement for silicone gels [63–65], and 4) combined geometrical techniques and applying nonlinear field-dependent conductivity layers [66–72].

A ferroelectric filler, barium titanate, was added in the base silicone gel to form an FDP stress-relieving dielectric material [62]. However, this technique has two limits, especially for WBG modules. First, the mentioned stress-relieving merit disappears above a specific temperature known as the Curie point. For pure barium titanate, this temperature is ∼130 °C [62]. Although the Curie point in a filled gel increases and is above the maximum junction temperature of Si-IGBT devices of 150 °C in the transistor and 125 °C in the diodes [62], this technique will probably have a serious issue in WBG modules, which may operate up to 200 °C, that is the limiting operating temperature of silicone gel and is targeted to 500 °C. Another issue is that an increase in the rate of the filler increases viscosity dramatically. In this regard, the viscosity of the filled gel with 15% barium titanate by volume increases by five times, which is a significant increase [62]. Although the filled composite was still capable of being poured and flowed well through the module [62], a rate of more than 15% by volume of barium titanate likely cannot be used due to the viscosity issue. It is crystal clear that this method has a critical thermal limitation for use in WBG-based power modules where the temperatures go beyond 200 °C.

Although the dielectric strength of a high temperature non-polar dibenzyltoluene (DBT) liquid, Jarytherm® DBT [73], proposed in [63–65] as an encapsulant in high-temperature power electronics modules is higher than other dielectric liquids, such as mineral oil or esters at 20 °C, its dielectric strength at 350 °C decreases to about 58% of its initial value at 20 °C. However, PD measurements in [65] shows promising results for these high temperature liquids as an alternative for silicone gel. To the best of our knowledge, there are only three papers [63–65] (all are conference papers) proposing DBT as an alternative for silicone gel for high-temperature WBG power modules. The low number of papers on this topic and their publication year (2018, 2019) indicates that this topic is very immature. However, all other mitigation methods try to address high electric field stress and this, using high-temperature dielectric liquids instead of silicone gel, is the only method proposed to date to address operating high temperatures. In our view, the high temperature issue, especially beyond 200 °C, will be much more challenging than the high electric field stress issue for next-generation WBG power modules. To address this, either new dielectrics, such as the DBD liquids mentioned above, will be examined, or advanced thermal management systems will be developed to keep the operating temperature inside WBG power modules lower than 200 °C, or a combination of two mentioned methods will be introduced.

Although nonlinear FDC materials known as resistive electric field grading materials have been used in stress grading systems in form-wound machines and in cable terminations [74, 75, to cite a few], these materials were first proposed in [61] for electric field grading for power electronics modules. However, they have not been used in practice to date.

The geometrical techniques for electric field reduction within power modules include 1) metal layer offset [56, 57], 2) protruding substrate [56, 58], 3) stacked substrate [59], and 4) 3D module layers [60]. In this regard, the 3D module layer method leads to an increase of 20% in stray inductance [60].

Studies in [66–72] prove that geometrical techniques including 1) metal layer offset, 2) protruding substrate, and 3) stacked substrate design, either individually or combined, cannot solve the high electric field issue in high voltage high-density WBG power modules. The use of a combination of the aforementioned geometrical methods and applying a nonlinear FDC layer were examined in [66–72]. The combination used for blocking voltages up to 30 kV addressed the issue well. Moreover, an electric field criterion based on precise dimensions of a power module and its PD measurement was introduced in [71]. To design the insulation systems for next-generation compact WBG power modules, [71, 72] can be used as guidelines to design the insulation system for next-generation compact WBG power modules, meeting both the one-minute insulation and PD tests based on IEC 61287-1 [76], which is the only existing standard for insulation performance of power electronics modules. It was shown that the proposed method brought E down to the criterion values

Authorized licensed use limited to: to IEEExplore provided by University Libraries | Virginia Tech. Downloaded on December 03,2021 at 03:46:18 UTC from IEEE Xplore. Restrictions apply.

well, and that an electric field reduction of 66 and 91% in AlN substrate and silicone gel, respectively could be achieved through the proposed method compared with using the protruding substrate design alone [72].

Both the one-minute insulation test and the PD test recommended in IEC 61287-1 are under 50/60 Hz sinusoidal voltage. According to IEC 61287-1 for PD measurement, a 50/60 Hz AC voltage with a maximum of $1.5U_b$, where U_b is the blocking voltage of the module, is applied for one minute (t_1), which is followed by a maximum AC voltage of $1.1U_b$ for 30 seconds (t_2). The detected PD level in the last 5 seconds of t_2 must not exceed 10 pC. IEC 61287-1 may be acceptable as long as the frequency and slew rate of voltage pulses in the power modules are not high. IEC 61287-1 does not provide a real situation for silicone gel and ceramic substrate as a consequence of exposure to the high slew rates (ranging from tens to hundreds of kV/µs) and repetitive (frequencies ranging from hundreds of kHz to MHz) voltage pulses that originate from emerging WBG-based power electronics systems. However, it should be noted that high-frequency noise due to switching activities of the voltage source generating fast, repetitive testing voltage pulses will reduce the test sensitively of the PD tests and determination of a proper bandwidth for the filter to reject the mentioned switching noises is a challenging task. In this regard, either technical issues regarding PD measurement under fast, repetitive voltage pulses should be investigated or a suitable coefficient instead of 1.1, and a suitable value for 10 pC in IEC 61287-1 should be found to represent real situations under fast, repetitive voltage pulses. This is a dramatic technical gap that needs urgent attention.

A critical review of the accelerated insulation aging issue, identifying technical gaps and future research needs, has recently been carried out in [77] where the main focus of that review paper is on the impact of fast, repetitive voltage pules on insulation systems in other electrification components such as electrical motors, transformers, cables, and solid-state transformers.

Simulations in [66–72] were done under 50 Hz sinusoidal AC voltage to meet IEC 61287-1. However, as mentioned before, in practice, the insulation materials of envisaged WBG power modules will be under square wave voltage pulses with frequencies up to a few kHz or MHz and temperatures up to a few hundred degrees. The relative permittivity and electrical conductivity of ceramic substrates, silicone gel, and nonlinear FDC materials assumed to be constant in [66–72] will be frequency- and temperature-dependent and their dependency should be considered in the model. In [78, 79], the frequency dependence of the mentioned parameters was considered based on measurement data reported in the literature. However, measurement data reported in the literature is for sinusoidal voltages with different frequencies. There is a technical gap here. We need to know how the relative permittivity and electrical conductivity of different insulating material used within power modules change with frequency under square waveform (not sinusoidal) voltages. Also, other factors of the square wave applied voltage such as slew rate, duty cycle, and polarity may affect relative permittivity and electrical conductivity. A comprehensive experimental investigation is needed to address this gap. This is the case for the temperature dependency of the mentioned parameter where the temperature within the future modules has been targeted up to 500°C. Then, a frequency- and temperature-dependent finite element method model of the insulation system must be developed for the envisioned high voltage, high-density WBG power modules.

Another technical gap and challenge is to develop advanced processing techniques to deposit thin layers of nonlinear FDC/FDP material with thicknesses ranging from a few ten to a few hundred µm. In this regard, an innovative method to tailor functionally graded materials by local handling of high permittivity ceramic particles of $SrTiO_3$ into epoxy resin using electrophoresis was reported in [80]. As shown in Figure 10, by applying a DC electric field onto the liquid composite compound, i.e., liquid epoxy resin with a hardener and $SrTiO_3$ particles, for 15 min before curing it in order to freeze the particles exactly where they have accumulated, the desired particle concentration gradient near the high voltage electrode was achieved. Details of the electrophoresis and curing process can be found in [80]. The thickness and distribution of the particles can be adjusted by controlling the electrophoretic force. As a result, the permittivity of the accumulated layer can be increased in value ranging between 22 and 24 in the frequency range under test.

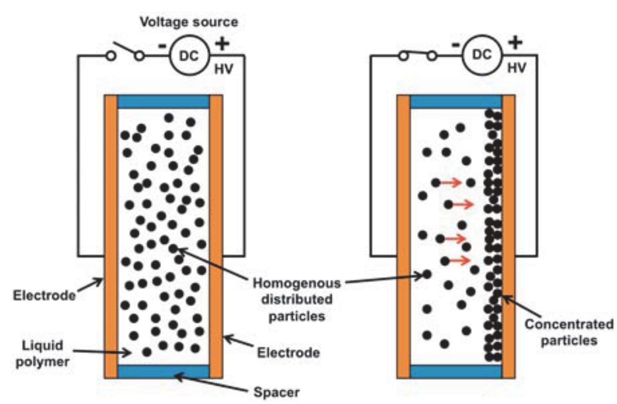

Figure 10. Electrophoresis process principle under DC voltage for structuring FGM polymer/ceramic composites [80], © [2018] IEEE.

This strategy was successfully applied to metalized DBC substrates used in power electronics modules. By applying DC voltage on the metalized Cu electrode during the curing process, an accumulated layer consisting of $SrTiO_3$ particles was formed, as shown in Figure 11. This high permittivity layer covers the Cu electrode, especially around the two sharp tips where the field enhancement is the highest. The efficiency of the method is shown by performing a field simulation in Figure 12.

The field enhancement at the triple point (i.e. the point where the ceramic substrate, copper electrode, and encapsulation material meet together) is significantly reduced

Authorized licensed use limited to: to IEEExplore provided by University Libraries | Virginia Tech. Downloaded on December 03,2021 at 03:46:18 UTC from IEEE Xplore. Restrictions apply.

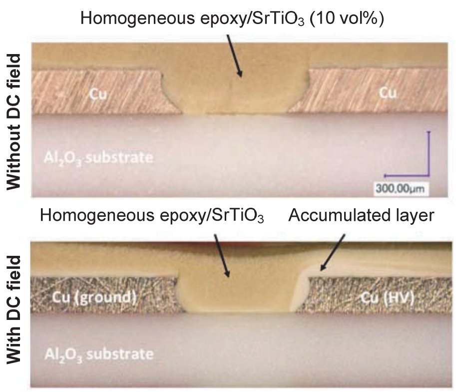

Figure 11. Application of the FGM to metalized alumina DBC substrates used in power electronics modules [80], © [2018] IEEE.

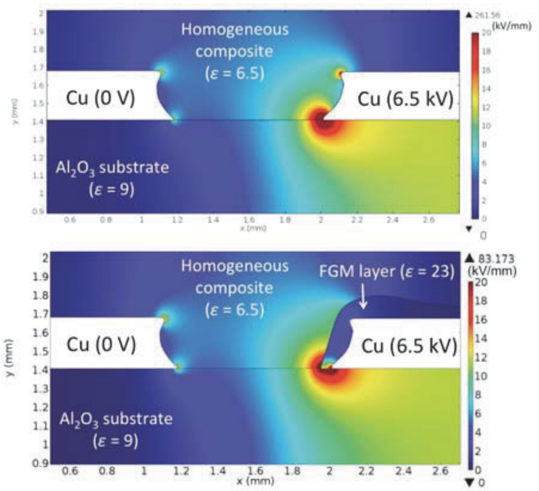

Figure 12. Electrostatic field simulations of the DBC structure with and without an FGM layer [80], © [2018] IEEE.

to only 1/3 of the original design. The breakdown tests also highlighted a 70% improvement in breakdown voltage compared to neat epoxy encapsulation. Such a field grading material (FGM) method, patented in France [81], can self-adaptively tailor the insulating materials and selectively heal the defects that occur during the system packaging assembly.

A field grading substrate was also proposed recently in [82], where the idea is to modify the part of the substrate ceramic at the triple point with higher conductivity. Figure 13 shows the impact of this field grading method on the electric field distribution by modifying the AlN conductivity by a factor of 1×10^6. The maximum electric field value is significantly reduced and occurs at region B, which is away from the triple point area.

In the geometric technique proposed in [83, 84], a gap between the top Cu electrodes was created to form a mesa structure, leading to significant electric field reduction as shown in Figure 14. This mesa structure was fabricated as shown in Figure 15 by an ultrasonic machining technique. Even though the machining introduces some protuberances on the upper corner of the Cu electrode, a 30% increase in the PD inception voltage (PDIV) was observed in the mesa structure compared to the conventional one.

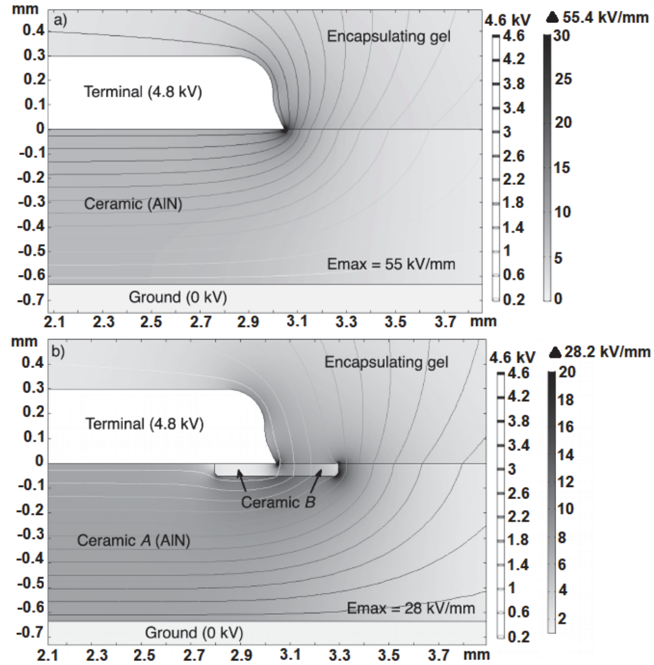

Figure 13. Field simulations of the (a) conventional DBC structure and (b) substrate with a higher conductivity in region B [82], © [2019] IEEE.

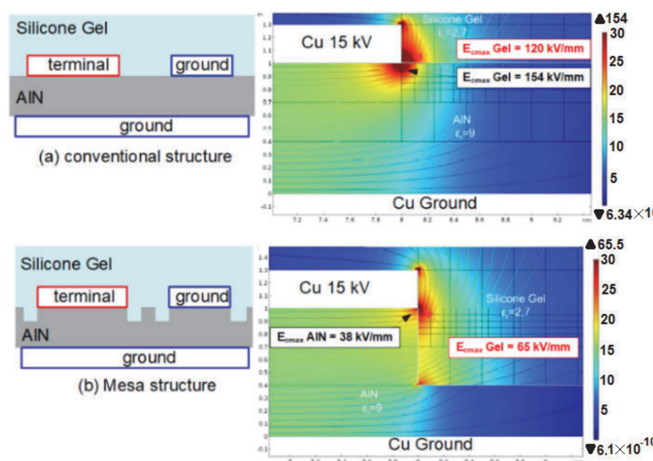

Figure 14. The geometry of (a) conventional structure and (b) mesa structure and the corresponding electric field distribution [83], © [2019] EPJ AP.

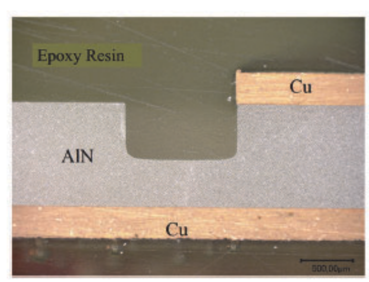

Figure 15. A cross-sectional view of the mesa structure built by ultrasonic machining [83], © [2019] EPJ AP.

As mentioned in the abstract, three factors are expected to lead to accelerated insulation aging within future WBG power modules. Each of these parameters plays an important role,

Authorized licensed use limited to: to IEEExplore provided by University Libraries | Virginia Tech. Downloaded on December 03,2021 at 03:46:18 UTC from IEEE Xplore. Restrictions apply.

and the key is that all three parameters exist at the same time. However, research results reported in the literature, both experimental work and model development, have considered only one of these parameters alone. In this regard, thermal stress, particularly, may play a major role in insulation degradation due to the high temperatures targeted up to 500°C. To date, this has not been sufficiently paid attention to.

Voltage surges with steep fronts, caused by turning semiconductor switches (power electronics modules) on/off in converters, travel through transmission lines or cables, and are reflected at interfaces due to impedance mismatches, giving rise to local overvoltages. Phenomena that are typically associated with these repetitive overvoltages are PDs and heating in insulation systems on the motor side, both of which contribute to insulation system degradation. Power electronics modules in inverters feeding the motor may experience such overvoltages or overshoots if cable lengths are short or generally for cases where the inverter is very close to the motor. However, to the best of our knowledge, this issue for power modules has not been reported.

5 CONCLUSIONS AND PERSPECTIVES

This paper presents a critical review of recent efforts to address the expected accelerated aging and degradation of insulation materials used within envisioned high voltage, high-density WBG power modules. Technical gaps and future research needs in two main areas were highlighted and discussed: 1) elucidating the mechanisms and phenomena behind prebreakdown in insulation materials employed within the mentioned power modules through both experimental investigation and modeling, and 2) developing mitigation methods. Combined geometrical techniques with nonlinear FDC materials applied to high electric field regions and using high temperature liquid dielectrics instead of silicone gel were highlighted as promising methods to address the high electric stress and high temperature issues, respectively. The existing standard, IEC 61287-1, for PD testing of power modules that use a 50/60 Hz sinusoidal voltage cannot simulate the real-world situation for insulation materials for future WBG power modules under high slew rates (ranging from tens to hundreds of kV/μs) and repetitive (frequencies ranging from hundreds of kHz to MHz) voltage pulses. Due to targeting the operation of these WBG power modules up to 500°C, thermal stress will play a critical role in insulation degradation and is needed to be considered both when developing a new standard for insulation testing of WBG power modules and when developing mitigation methods.

REFERENCES

[1] U.S. Department of Energy, Electricity Delivery and Energy Reliability, “Power electronics research and development, program plan,” 2011.

[2] B. Passmore and C. O’Neal, “High-voltage SiC power modules for 10–25 kV applications,” Power Electron. Europe Mag., no. 1, pp. 22–24, 2016.

[3] P. Wang, G. C. Montanari, and A. Cavallini, “Partial discharge phenomenology and induced aging behavior in rotating machines controlled by power electronics,” IEEE Trans. Ind. Electron., vol. 61, no. 12, pp. 7105–7112, 2014.

[4] P. Wang, A. Cavallini, and G. C. Montanari, “The influence of repetitive square wave voltage parameters on enameled wire endurance,” IEEE Trans. Dielectr. Electr. Insul., vol. 21, no. 3, pp. 1276–1284, 2014.

[5] A. Cavallini, “Reliability of low voltage inverter-fed motors: What have we learned, perspectives, open points,” *IEEE Int. Symp. Electr. Insul. Materials (ISEIM)*, 2017, pp. 13–22.

[6] M. Ghassemi, “PD measurements, failure analysis, and control in high power IGBT modules,” High Voltage, vol. 3, no. 3, pp. 170–178, 2018.

[7] M. Ghassemi, “Electrical insulation weaknesses in wide bandgap devices,” in *Simulation and Modelling of Electrical Insulation Weaknesses in Electrical Equipment*, R. Albarracin Ed. London, U.K.: InTechOpen, 2018, pp. 129–149.

[8] S. J. Dodd *et al*, “Electrical trees in silicone gel: a combination of liquid and solid behaviour patterns,” *Annu. Rep. Conf. Electr. Insul. Dielectr. Phenom. (CEIDP)*, 2013, pp. 1018–1021.

[9] L. A. Dissado and J. C. Fothergill, *Electrical Degradation and Breakdown in Polymers*, Peter Peregrinus Ltd., London, United Kingdom, 1992.

[10] Y. Zhang *et al* “DC electrical tree initiation in silicone rubber under temperature gradient,” IEEE Trans. Dielectr. Electr. Insul., vol. 25, no. 3, pp.1142–1150, 2018.

[11] K. Wu and L. A. Dissado “Model for electrical tree initiation in epoxy resin,” IEEE Trans. Dielectr. Electr. Insul., vol. 12, no. 4, pp. 655–668, 2005.

[12] A. S. Vaughan *et al*, “On the structure and chemistry of electrical trees in polyethylene,” J. Phys. D. Appl. Phys., vol. 39, no. 5, pp. 962–978, 2006.

[13] P. Tiemblo *et al* “The development of electrical treeing in LDPE and its nanocomposites with spherical silica and fibrous and laminar silicates,” J. Phys. D. Appl. Phys., vol. 41, no. 12, pp. 1–8, 2008.

[14] Y. Zhou *et al* “Morphology of electrical trees in silicon rubber,” J. Electrostat., vol.71, no. 3, pp. 440–448, 2013.

[15] P. Mancinelli *et al*, “Analysis of electrical tree inception in silicone gels,” IEEE Trans. Dielectr. Electr. Insul., vol. 24, no. 6, pp. 3974–3984, 2017.

[16] L. M. Salvatierra *et al*, “Self-healing during electrical treeing: a feature of the two-phase liquid-solid nature of silicone gels,” IEEE Trans. Dielectr. Electr. Insul., vol. 23, no. 2, pp. 757–767, 2016.

[17] P. Gournay and O. Lesaint, “On the gaseous nature of positive filamentary streamers in hydrocarbon liquids. II: Propagation, growth and collapse of gaseous filaments in pentane,” J. Phys. D: Appl. Phys., vol. 27, pp. 2117–2127, 1994.

[18] A. Beroual *et al*, “Propagation and structure of streamers in liquid dielectrics,” IEEE Electr. Insul. Mag., vol. 14, no. 2, pp. 16–17, 1998.

[19] H. Akiyama, “Streamer discharges in liquids and their applications,” IEEE Trans. Dielectr. Electr. Insul., vol. 7, no.5, pp. 646–652, 2000.

[20] P. K. Watson, W. G. Chadband, M. Sadeghzadeh-Araghi, “The role of electrostatic and hydrodynamic forces in the negative point breakdown in liquid dielectrics,” IEEE Trans. Dielectr. Electr. Insul., vol. 26, pp. 543–559, 1991.

[21] T. Aka-Ngnui and A. Beroual, “Bubble dynamics and transition into streamers in liquid dielectrics under a high divergent electric field,” J. Phys. D: Appl. Phys., vol. 34, pp. 1408–1412, 2001.

[22] T. M. Do, O. Lesaint, and J. L. Augé, “Streamers and partial discharge mechanisms in silicone gel under impulse and AC voltages,” IEEE Trans. Dielectr. Electr. Insul., vol. 15, no. 6, pp. 1526–1534, 2008.

[23] T. M. Do, J. L. Augé, and O. Lesaint, “A study of parameters influencing streamer inception in silicone gel,” IEEE Trans. Dielectr. Electr. Insul., vol. 16, no. 3, pp. 893–899, 2009.

[24] A. Beroual *et al*, “Propagation and structure of streamers in liquid dielectrics,” IEEE Electr. Insul. Mag., vol. 14, no. 2, pp. 16–17, 1998.

[25] H. Akiyama, “Streamer discharges in liquids and their applications,” IEEE Trans. Dielectr. Electr. Insul., vol. 7, no. 5, pp. 646–652, 2000.

[26] T. M. Do, O. Lesaint, and J. L. Augé, “Streamers and partial discharge mechanisms in silicone gel under impulse and AC voltages,” IEEE Trans. Dielectr. Electr. Insul., vol. 15, no. 6, pp. 1526–1534, 2008.

[27] M. Sato *et al*, “Degradation Process of silicone-gel by internal surface discharges,” *IEEE Int. Conf. Dielectr. Liquids (ICDL)*, 2014, pp. 1–4.

[28] M. Sato *et al*, “Viscoelastic analysis of cavity propagation in gel with electrical discharge,” J. Phy. D: Appl. Phys., vol. 47, p. 55201, 2014.

[29] T. Ebke, A. Khaddour, and D. Pier, “Degradation of silicone gel by partial discharges due to different defects,” *Int. Conf. Dielectr. Materials, Meas. Appl.*, 2000, pp. 202–207.

[30] M. Sato *et al*, “On the nature of surface discharges in silicone-gel: Pre-breakdown discharges in cavities,” *Annu. Rep. Conf. Electr. Insul. Dielectr. Phenom. (CEIDP)*, 2014, pp. 19–22.

Authorized licensed use limited to: to IEEExplore provided by University Libraries | Virginia Tech. Downloaded on December 03,2021 at 03:46:18 UTC from IEEE Xplore. Restrictions apply.

[31] M. Sato *et al*, "Dynamic potential distributions of surface discharge in silicone gel," IEEE Trans. Dielectr. Electr. Insul., vol. 22, no. 3, pp. 1733–1738, 2015.

[32] L. A. Dissado. "Understanding electrical trees in solids: from experiment to theory," IEEE Trans. Dielectr. Electr. Insul., vol. 9, no. 4, pp.483–497, 2002.

[33] B. X. Du *et al*, "Effect of ambient temperature on electrical treeing characteristics in silicone rubber," IEEE Trans. Dielectr. Electr. Insul., vol. 18, no. 2, pp. 401–407, 2011.

[34] X. R. Chen *et al*, "Electrical treeing behavior at high temperature in XLPE cable insulation samples," IEEE Trans. Dielectr. Electr. Insul., vol. 22, no. 5, pp. 2841–2851, 2015.

[35] R. H. Fowler and L. Nordheim, "Electron emission in intense electric fields," Proc. Roy. Soc., vol. 119, pp. 173–181, 1928.

[36] H. Fröhlich, "On the theory of dielectric breakdown in solids," Proc. Roy. Soc., vol. 188, no. 1015, pp. 521–532, 1947.

[37] T. Yamakita. "Temperature dependence of superstructure and electrical tree initiation voltage of polyethylene," Electr. Eng. in Japan, vol. 128, no. 33, pp. 24–30, 1999.

[38] Y. Zhang *et al*, "Temperature dependence of DC electrical tree initiation in silicone rubber considering defect type and polarity," IEEE Trans. Dielectr. Electr. Insul., vo. 24, no. 5, pp. 2694-2702, 2017.

[39] H. Ejiri *et al*, "The influence of frequency and rise time of applied voltage upon cavity propagation in silicone gel," *Int. Conf. Gas Discharges Appl.*, 2016, pp. 309–312.

[40] S. Nakamura *et al*, "Cavity propagation under repetitive voltage impulses in silicone gel for encapsulation of power modules," *IEEE Int. Conf. Dielectr. (ICD)*, 2018, pp. 1–4.

[41] S. Nakamura *et al*, "Electrical treeing in silicone gel under repetitive voltage impulses," IEEE Trans. Dielectr. Electr. Insul., vol. 26, no. 6, pp. 1919–1925, 2019.

[42] Y. Zhang *et al* "Electrical trees and their growth in silicone rubber at various frequencies," Energies, vol. 11, no. 2, pp. 327–338, 2018.

[43] J. -L. Auge, O. Lesaint, and A. T. V. Thi, "Partial discharges in ceramic substrates embedded in liquids and gels," IEEE Trans. Dielectr. Electr. Insul., vol. 20, no. 1, pp. 262–274, 2013.

[44] M. Sato *et al*, "Surface discharges in silicone gel on AlN substrate," IEEE Trans. Dielectr. Electr. Insul., vol. 23, no. 1, pp. 494–500, 2016.

[45] S. Whitehead, Dielectric Breakdown in Solids, Oxford: Clarendon Press, 1951.

[46] G. Callender *et al*, "Critical analysis of partial discharge dynamics in air filled spherical voids," J. Phys. D: Appl. Phys., vol. 51, no.12, 2018.

[47] G. Callender, T. Tanmaneeprasert, and P. L. Lewin, "Simulating partial discharge activity in a cylindrical void using a model of plasma dynamics," J. Phys. D: Appl. Phys., vol. 52, no. 5, 2019.

[48] M. Borghei *et al*, "A finite element analysis and an improved induced charge concept for partial discharge modeling," IEEE Trans. Power Del., to be published, DOI: 10.1109/TPWRD.2020.2991589

[49] H. A. Illias, G. Chen and P. L. Lewin, "Comparison between three-capacitance, analytical-based and finite element analysis partial discharge models in condition monitoring," IEEE Trans. Dielectr. Electr. Insul., vol. 24, no. 1, pp. 99–109, 2017.

[50] C. Forssen and H. Edin, "Partial discharges in a cavity at variable applied frequency part 2: measurements and modeling," IEEE Trans. Dielectr. Electr. Insul., vol. 15, no. 6, pp. 1610–1616, 2008.

[51] L. Niemeyer, "A generalized approach to partial discharge modeling," IEEE Trans. Dielectr. Electr. Insul., vol. 2, no. 4, pp. 510–528, 1995.

[52] F. Gutfleisch and L. Niemeyer, "Measurement and simulation of PD in epoxy voids," IEEE Trans. Dielectr. Electr. Insul., vol. 2, no. 5, pp. 729–743, 1995.

[53] M. Borghei and M. Ghassemi, "Partial discharge analysis under high-frequency, fast-rise square wave voltages in silicone gel: A modeling approach," Energies, vol. 12, no. 23, p. 4543, 2019.

[54] M. Borghei and M. Ghassemi, "Finite element modeling of partial discharge activity within a spherical cavity in a solid dielectric material under fast, repetitive voltage pulses," *IEEE Electr. Insul. Conf. (EIC)*, 2019, pp. 34–37.

[55] M. Borghei and M. Ghassemi, "Partial discharge finite element analysis under fast, repetitive voltage pulses," *IEEE Electr. Ship Technol. Symp. (ESTS)*, 2019, pp. 324–328.

[56] M. Ghassemi, "Geometrical techniques for electric field control in (Ultra) wide bandgap power electronics modules," *IEEE Electr. Insul. Conf. (EIC)*, 2018, pp. 589–592.

[57] C. F. Bayer *et al*, "Simulation of the electric field strength in the vicinity of metallization edges on dielectric substrates," IEEE Trans. Dielectrics Electr. Insul., vol. 22, no. 1, pp. 257–265, 2015.

[58] H. Reynes, C. Buttay, and H. Morel, "Protruding ceramic substrates for high voltage packaging of wide bandgap semiconductors," *IEEE Workshop Wide Bandgap Power Devices Appl. (WiPDA)*, 2017, pp. 404–410.

[59] O. Hohlfelder *et al*, "Stacked substrates for high voltage applications," *Int. Conf. Integr. Power Electron. Syst. (CIPS)*, 2012, pp. 1–4.

[60] D. Frey *et al*, "Electric field investigation in high voltage power modules using finite element simulations and partial discharge measurements," *IEEE Conf. Ind. Appl. Soc. Annu. Meeting (IAS)*, 2003, pp. 1000–1005.

[61] L. Donzel and J. Schuderer, "Nonlinear resistive electric field control for power electronic modules," IEEE Trans. Dielectr. Electr. Insul., vol. 19, no. 3, pp. 955–959, 2012.

[62] N. Wang *et al*, "Partial discharge control in a power electronic module using high permittivity non-linear dielectrics," IEEE Trans. Dielectr. Electr. Insul., vol. 17, no. 4, pp. 1319–1326, 2010.

[63] D. J. Muslim *et al*, "Electrical characterization of dibenzyltoluene liquid at high temperatures up to 350 °C," *Annu. Rep. Conf. Electr. Insul. Dielectr. Phenom. (CEIDP)*, 2018, pp. 58–61.

[64] J. Muslim *et al*, "Streamer generation and propagation in Dibenzyltoluene and Ester liquids under high temperature," *IEEE Int. Conf. Dielectr. Liquids (ICDL),* 2019, pp. 1–4.

[65] J. Muslim *et al*, "Partial discharge measurements on Dibenzyltoluene for high temperature encapsulant application up to 350°C," *IEEE Int. Conf. Dielectr. Liquids (ICDL),* 2019, pp. 1–4.

[66] M. M. Tousi and M. Ghassemi, "Electric field control by nonlinear field dependent conductivity dielectrics characterization for high voltage power module packaging," *IEEE Int. Workshop Integr. Power Packag. (IWIPP)*, 2019, pp. 54–58.

[67] M. M. Tousi and M. Ghassemi, "Nonlinear field dependent conductivity materials for electric field control within next-generation wide bandgap power electronics modules," *IEEE Electr. Insul. Conf. (EIC)*, 2019, pp. 63–66.

[68] M. M. Tousi and M. Ghassemi, "Nonlinear resistive electric field grading in high-voltage, high-power wide bandgap power module packaging," *IEEE Energy Convers. Congr. Expo. (ECCE)*, 2019, pp. 7124–7129.

[69] M. M. Tousi and M. Ghassemi, "Electrical insulation packaging for a 20-kV high density wide bandgap power module," *IEEE Energy Convers. Congr. Expo. (ECCE)*, 2019, pp. 4162–4166.

[70] M. M. Tousi and M. Ghassemi, "The effect of type of voltage (sinusoidal and square waveform) and the frequency on the performance of nonlinear field-dependent conductivity coatings for electric field control in power electronic modules," *Annu. Rep. Conf. Electr. Insul. Dielectr. Phenom. (CEIDP)*, 2019, pp. 601–604.

[71] M. M. Tousi and M. Ghassemi, "Combined geometrical techniques and applying nonlinear field dependent conductivity layers to address the high electric field stress issue in high voltage high-density wide bandgap power modules," IEEE Trans. Dielectr. Electr. Insul., vol. 27, no. 1, pp. 305–313, 2020.

[72] M. M. Tousi and M. Ghassemi, "Nonlinear field dependent conductivity for electric field grading in wide bandgap power electronic modules," IEEE J. Emerg. Sel. Topics Power Electron., vol. 8, no. 1, pp. 343–350, 2020.

[73] Jarytherm® DBT, Available: https://www.arkema.coexport/shared/content/media/downloads/products-documentations/hydrogen-peroxide/Jarytherm-DBT-TDS.pdf

[74] A. Naeini, E. A. Cherney, and S. H. Jayaram, "Effect of conductivity on the thermal and electrical properties of the stress grading system of an inverter-fed rotating machine," IEEE Trans. Dielectr. Electr. Insul., vol. 26, no. 1, pp. 179–186, 2019.

[75] F. P. Espino-Cortes, S. Jayaram, and E. A. Cherney, "Stress grading materials for cable terminations under fast rise time pulses," IEEE Trans. Dielectr. Electr. Insul., vol. 13, no. 1, pp. 430–435, 2006.

[76] Railway applications – power converters installed on board rolling stock – part 1: characteristics and test methods, IEC 61287-1: 2014, 2014-07-10

[77] M. Ghassemi, "Accelerated insulation aging due to fast, repetitive voltages: A review identifying challenges and future research needs," IEEE Trans. Dielectr. Electr. Insul., vol. 26, no. 5, pp. 1558–1568, 2019.

[78] M. M. Tousi and M. Ghassemi, "Effects of frequency and temperature on electric field mitigation method via protruding substrate combined

Authorized licensed use limited to: to IEEExplore provided by University Libraries | Virginia Tech. Downloaded on December 03,2021 at 03:46:18 UTC from IEEE Xplore. Restrictions apply.

with applying nonlinear FDC layer in wide bandgap power modules," *Energies*, vol. 13, no. 8, p. 2022, April 2020.
[79] M. M. Tousi and M. Ghassemi, "Influence of Temperature and Frequency on Electric Field Reduction Method via a Nonlinear Field Dependent Conductivity Layer Combined with Protruding Substrate for Power Electronics Modules," *IEEE Electrical Insulation Conference (EIC)*, 2020, accepted.
[80] S. Diaham *et al*, "An original in-situ way to build field grading materials (FGM) with permittivity gradient using electrophoresis," *IEEE Int. Conf. Dielectr. (ICD)*, 2018, pp. 1–4.
[81] S. Diaham *et al*, "Procédé de traitement d'un matériau électriquement isolant lui conférant des propriétés de gradation de champ électrique auto-adaptatives pour composants électriques," Int. Patent application, N° PCT/EP2017/063740, CNRS/UPS/INUC, 6 June 2017-French Patent application, N° FR 16 55173, CNRS/UPS/INUC, 6 June 2016.
[82] Z. Valdez-Nava *et al*, "Ceramic substrates for high voltage power electronics: past, present and future," *IEEE Int. Workshop Integr. Power Packag. (IWIPP)*, 2019, pp. 91–96.
[83] H. Hourdequin *et al*, "Metallized ceramic substrate with mesa structure for voltage ramp-up of power modules," Eur. Phys. J. Appl. Phys., vol. 87, p. 20903, 2019.
[84] H. Hourdequin *et al*, "Design of packaging structures for high voltage power electronics devices: electric field stress on insulation," *IEEE Int. Conf. Dielectr. (ICD)*, 2016, pp. 999–1002.

Boya Zhang (M'16) was born in Xi'an, China in 1990. He received the B.Sc. degree and Ph.D. degree in electrical engineering from Tsinghua University, Beijing, China in 2013 and 2018, respectively. From 2016–2017, he worked at the Electrical Insulation Research Center, Institute of Materials Science, University of Connecticut, Storrs, CT, USA as a research scholar. Currently, he is an assistant professor at School of Electrical Engineering at Xi'an Jiaotong University. His research interests cover insulation materials and systems, high voltage and large current technology, power equipment modeling and design, gas discharge and plasma.

Mona Ghassemi (S'07–M'13–SM'16) received her M.Sc. and Ph.D. degrees (Hons.) in electrical engineering from the University of Tehran, Tehran, Iran, in 2007 and 2012, respectively. She spent two years (2013–2015) researching as a Post-Doctoral Fellow at the High Voltage Laboratory of the University of Quebec, QC, Canada. She was also a Post-Doctoral Fellow at the Electrical Insulation Research Center, Institute of Materials Science, University of Connecticut, Storrs, CT, USA, from 2015 to 2017. In 2017, she joined the ECE Department at Virginia Tech (Blacksburg, VA, USA) as an assistant professor. Dr. Ghassemi is an At-Large Member of the Administrative Committee of the IEEE Dielectrics and Electrical Insulation Society for 2020–2023, a Corresponding Member of the IEEE Conference Publication Committee of the IEEE Power & Energy Society, an Active Member of several CIGRE working groups and IEEE Task Forces, and a member of the Education Committee of the IEEE DEIS and PES. She is a registered Professional Engineer in the Province of Ontario, Canada, and an Associate Editor of the *IEEE Transactions on Industry Applications,* the *IET High Voltage,* and the *International Journal of Electrical Engineering Education*. She is also a recipient of the 2020 National Science Foundation (NSF) CAREER Award and the 2020 Air Force Office of Scientific Research (AFOSR) Young Investigator Research Program (YIP) Award. Her research interests include electrical insulation materials and systems, high voltage/field technology, Multiphysics modeling, electromagnetic transients in power systems, and power system analysis and modeling.

Yunxiao Zhang was born in Fujian Province, China in 1990. He received the B.Sc. degree and Ph.D. degree in electrical engineering in 2013 and 2018 from Tsinghua University, China. He worked at Department of Engineering in Leicester University, UK as a research scholar in 2017. Currently, he is an assistant research fellow in Tsinghua University. His research interests include new insulation materials design, advanced insulating measurement technology, and aging phenomenon in solid insulation materials.

Authorized licensed use limited to: to IEEExplore provided by University Libraries | Virginia Tech. Downloaded on December 03,2021 at 03:46:18 UTC from IEEE Xplore. Restrictions apply.